Jestr

Journal of Engineering Science and Technology Review 13 (5) (2020) 193 - 198

JOURNAL OF
Engineering Science and Technology Review

Research Article

www.jestr.org

Influence of Lateral Monotonic Loading Upon the Behaviour of Rubberized Concrete Filled Steel Tube

Abdullah Al-Shwaiter[1], Hanizam Awang[1,*] and Ziyad Al-Gaboby[2]

[1]*School of Housing, Building, and Planning, Universiti Sains Malaysia*
[2]*Engineering Department, Faculty of Engineering, University of Science and Technology*

Received 23 July 2020; Accepted 21 August 2020

Abstract

Using waste tyres as recycle material in the construction industry seems to be a good solution to the problem of waste management and landfill. The main purpose of this paper is to study the behaviour of rubberized concrete-filled steel tube (RuCFST) analytically for square and rectangular columns under lateral monotonic loading. Seventy-two prototypes modelled using ABAQUS 6.12-1 software with various variables, which are cross-section shape, rubber replacement as a percentage of natural aggregate, column length, sections slenderness ratio and the axial loading level. The results showed that the adopted model in elastic and plastic properties gives a good agreement between numerical and referenced experimental results. Moreover, increasing the rubber replacement percentage has no major effect on the columns' capacity; meanwhile increasing the columns' length lead to decrease the strength capacity dramatically. Furthermore, increasing the axial loading percentage leads to reduce the column lateral strength. Similarly, the columns' capacity decreases with increasing the section slenderness ratio.

Keywords: Rubberized concrete, Long column, infilled steel tube, FEM, recycle waste tyres, elastic and plastic properties.

1. Introduction

Owing to the several advantages that concrete offers, concrete is the most material used in construction projects [1]. Therefore, replacing concrete's row constituent by waste materials is an adequate solution to reduce the environment impacts. Many types of waste materials has been used in production of concrete including waste tyres, waste glass, waste plastic, and agriculture wastes [2, 3].

Every year the numbers of waste tyres have been increased. Nowadays, more than one billion tyres have reached the end of their useful lives around the world and this number has increased every year and expected to reach 1.5 billion by 2030 [4]. Moreover, about 3.5 million tons of waste tyres reach out of service in Euro countries alone [5] and in the USA about 2.5 billion tyres deposited in landfills yearly [6]. By using tyres in the concrete industry is helping to decrease the environmental impacts as well as conserving the natural resources.

Since using rubber in concrete reduces the mechanical properties of concrete [7], the crumb rubber always used as a partial replacement from natural aggregate or cement. Regardless the limited using of rubberized concrete in structural elements, rubberized concrete used widely in non-structural elements including barriers, block, panels, pavements, etc. [8-11]. On the other hand, concrete-filled steel tube (CFST) column is one of the most suitable solutions in the construction industry, forasmuch as high capacity to carry loads, high stability and small dimension comparing with traditional concrete or steel structure. In CFST the steel confined the concrete and enhance its compression resistance. Meanwhile, the concrete increases the steel strength to inhabit local buckling which provides high stiffness to resist lateral loads and decrease the total drift [12]. Moreover, the steel working as a framework which speed-up the construction time and decreases the costs.

Several studies carried out on the behavior of rubberized concrete with different rubber percentages. In general, increasing the rubber percentage in concrete reduce the workability, density, compression, tension, flexural capacity and modulus of elasticity of concrete [11, 13-17]. In contrast, using rubber in concrete enhance the ductility, impact resistance, sound insulation, energy dissipation, damping properties, and fracture [18-23]. Under dynamic compression, Pham, Chen [24] recorded that RuC reduce remarkably the crack propagation and showed progressive failure, as well, the specimens kept intact after test. Moreover, in concrete beams, it has been stated that increasing rubber content enhanced the impact resistance and reduced the static bending load, meanwhile, better toughness and deformation were observed [25, 26].

Many studies investigated the effect of different types of confinement under axial and lateral loading on the RuC columns behavior. The results showed that the increasing of the rubber content lead to decrease the strength, although the axial strain, lateral strain, impact energy absorption have increased [27, 28]. Moreover, Son, Hajirasouliha [29] stated that rubberized concrete columns show a lower compression capacity and modulus of elasticity and higher lateral deformation before the buckling failure occur. Meanwhile, Youssf, ElGawady [30] indicated that rubberized columns under seismic behavior presented a marginal reduction on the ultimate lateral strength and viscous damping ratio, however, both of energy dissipation and hysteretic damping ratio have been increased. In addition, there is no significant effect on

*E-mail address: hanizam@usm.my
ISSN: 1791-2377
doi:10.25103/jestr. 135.25

the strength of rubberized concrete columns while the lateral drift increases 12.5% at content 20% of rubber comparing with conventional columns [31].

Study on the RuCFST short columns subjected to axial loading shown that the compression capacity of columns decreases gradually with increase of rubber content [32, 33]. RuCFST columns subjected to lateral monotonical loading show no significant losses with increasing the rubber content [34, 35], although the RuCFST show a small reduction in the capacity under cyclic loading [34]. Under elevated temperature, replacing sand by crumb rubber led into lowered the mechanical properties of RuCFST [36]. In comparison with the previous studies, which are focused on the behavior of CFST in short columns, this study aims to study the effect of the length of CFST filled by rubberized concrete under lateral monotonical loading with and without axial loading. In addition, the effect of rubber content, slenderness ratio, and column shape for these columns were also been investigated.

2. Model Parameters

Seventy-two prototypes were modeled and analyzed by using ABAQUS 6.12-1 software. Several variables were used; exhaustively the column's length, rubber content, section's shape, section's slenderness ratio, and loading pattern. Two lengths used to meet the limits of AISC [37] requirements for short and long column. Two different cross-section shapes used which are square (200x200mm) and rectangular (300x133mm), and three rubber contents (0%, 5%, and 15%). Two slenderness ratios used to accomplish AISC requirement [37] for compact and slender sections. The loading is divided into three patterns based on the axial loading rate. These patterns are the pure lateral monotonic load (M0), the monotonic loading with constant axial load equal 20% and 50% from the columns' axial capacity. The columns cross-section are presented in Fig. **1**.

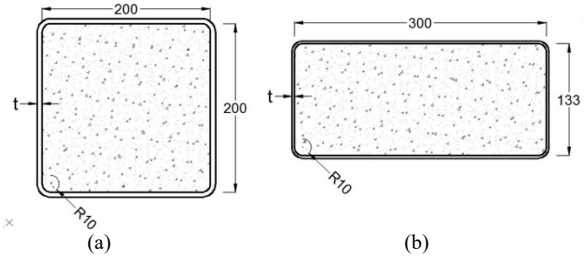

Fig. 1. Columns' cross section. a) square column, b) rectangular column

Table 1 presents the symbols and the parameters of this study; in which the symbol (S) used for square cross-section and (R) for rectangular cross-section. Also, the symbols (SH and L) used for short and long columns respectively, while the tube thickness 3.0 mm express the slender cross-section and 6.0 mm express the compacted cross-sections. In order to shorten Table 1, each row includes three specimens, Ru0%, Ru5%, and Ru15%.

Table 1. Specimens of the study

Specimen ID	High (m)	t (mm)	Axial load %	Ru%			Specimen ID	High (m)	t (mm)	Axial load %	Ru%		
S3-M0-SH-Ru(0,5,15)	1.5	3	0	0	5	15	R3-M0-SH-Ru(0,5,15)	1.5	3	20	0	5	15
S3-M0-L- Ru(0,5,15)	3	3	0	0	5	15	R3-M0-L- Ru(0,5,15)	3	3	20	0	5	15
S6-M0-SH- Ru(0,5,15)	1.5	6	0	0	5	15	R6-M0-SH- Ru(0,5,15)	1.5	6	20	0	5	15
S6-M0-L- Ru(0,5,15)	3	6	0	0	5	15	R6-M0-L- Ru(0,5,15)	3	6	20	0	5	15
R3-M0-SH-Ru(0,5,15)	1.5	3	0	0	5	15	S3-M0-SH-Ru(0,5,15)	1.5	3	50	0	5	15
R3-M0-L- Ru(0,5,15)	3	3	0	0	5	15	S3-M0-L- Ru(0,5,15)	3	3	50	0	5	15
R6-M0-SH- Ru(0,5,15)	1.5	6	0	0	5	15	S6-M0-SH- Ru(0,5,15)	1.5	6	50	0	5	15
R6-M0-L- Ru(0,5,15)	3	6	0	0	5	15	S6-M0-L- Ru(0,5,15)	3	6	50	0	5	15
S3-M0-SH-Ru(0,5,15)	1.5	3	20	0	5	15	R3-M0-SH-Ru(0,5,15)	1.5	3	50	0	5	15
S3-M0-L- Ru(0,5,15)	3	3	20	0	5	15	R3-M0-L- Ru(0,5,15)	3	3	50	0	5	15
S6-M0-SH- Ru(0,5,15)	1.5	6	20	0	5	15	R6-M0-SH- Ru(0,5,15)	1.5	6	50	0	5	15
S6-M0-L- Ru(0,5,15)	3	6	20	0	5	15	R6-M0-L- Ru(0,5,15)	3	6	50	0	5	15

Table 2 shows the steel mechanical properties that used in the simulation including the yield strength f_y, ultimate strength f_u, modulus of elasticity E_s and Poisson's ratio v_s. The standard value for Poisson's ratio 0.3 has been used.

Table 2. Steel Properties

Steel Grade	Fy (MPa)	Fu (MPa)	Es (GPa)	v_s
S235	284	403	200	0.3

Steel tube has been modeled as 3D deformable shell extrude element and the material was defined for elastic and plastic. The elastic behavior defined as an isotropic with young modulus equal 200 GPa and 0.3 for Poisson's ratio; whilst the plastic behavior is isotropic and the stress-strain values took from the experimental study [34] with eliminating the plastic stage. The steel section was defined as a homogeneous shell with integration during analysis [38]. The thickness values defined as 3mm and 6mm for slender and compacted cross-section respectively.

Table 3 shows the mechanical properties for the three rubber replacement percentage including the cube compression strength f_{cu} [34], splitting tension strength f_{ct}, modulus of elasticity E_c, elastic strain gauge value εc and Poisson's ratio ν. Although the Poisson's ratio of Ru0% assumed 0.2, Poisson's ratio of Ru5% and Ru15% calculated by using the admixture rule [39].

Table 3. Concrete mechanical properties

Concrete ID	f_c (MPa)	Ec (GPa)	f_{ct} (MPa)	εc	ν
Ru0%	53.0	38.0	3.5	0.2	0.2
Ru5%	39.0	33.5	2.6	0.42	0.21
Ru15%	20.0	25.2	2.0	0.54	0.23

Table 4. The parameters of Concrete Damaged Plasticity model CDP

Concrete type	ψ	Eccentricity	σ_{b0}/σ_{c0}	K	μ
NC	15	0.1	1.16	0.67	0.0002
Ru5%	7.5	0.1	1.16	0.67	0.0002
Ru15%	5	0.1	1.16	0.67	0.0002

The concrete part drew as 3D deformable extrusion solid with homogeneous solid section [38]. The elastic behavior defined as an isotropic with young modulus and Poisson's as shown in Table 3. The plastic behavior of concrete modeled by using concrete damage plasticity theory (CDP), which is based on Drucker-Prager hyperbolic function. This theory used since its ability to model the inelastic behavior of quasi-brittle materials like concrete. There are several parameters that are required to define the CDP model which are dilation angel (ψ), the flow potential eccentricity of the hyperbolic function (e), the ratio of compression strength under biaxial loading to uniaxial compressive strength (fb0/fc0), the ratio of the second stress invariant on the tensile meridian to that on the compressive meridian (Kc) and viscosity parameter (μ). Table 4 presents the CDP parameters, which cannot be obtainable from testing the concrete directly. Finally, the concrete's compression and tension behavior defined in CDP model defined based on the Eurocode 2 Johnson and Anderson [40] proposal.

A displacement toward +Z direction had been used to simulate the lateral loading at the top surface of concrete core and steel tube. At the same time, axial loading applied on top reference point along Y-axis toward the bottom of the column. Although the bottom of the concrete and steel tube restrained against all displacements and all rotational transitions along (X, Z, and Y) axis. In contrast, the transitions of all axes at the top part of the column were free. The interaction contact behavior was hard contact between steel tube and concrete core with allowing separation after contact for the lower 200m. The separation was allowed only at the bottom part since there was not any noticeable deformation existed on the top part based on experimental observation [34]. The friction coefficient in tangential behavior is 0.25 for both top and bottom parts.

The mesh of the column has been divided into two parts. The top part meshed with 20 and 45 layers along column length for short and long column respectively. The bottom part meshed to 12 layers along column length for both short and long columns. Moreover, the value 20 was adopted to divide both concrete and steel parameters in square columns and 22 is the value that was selected for rectangular columns. Fig 2 presents the mesh of square and rectangular short columns.

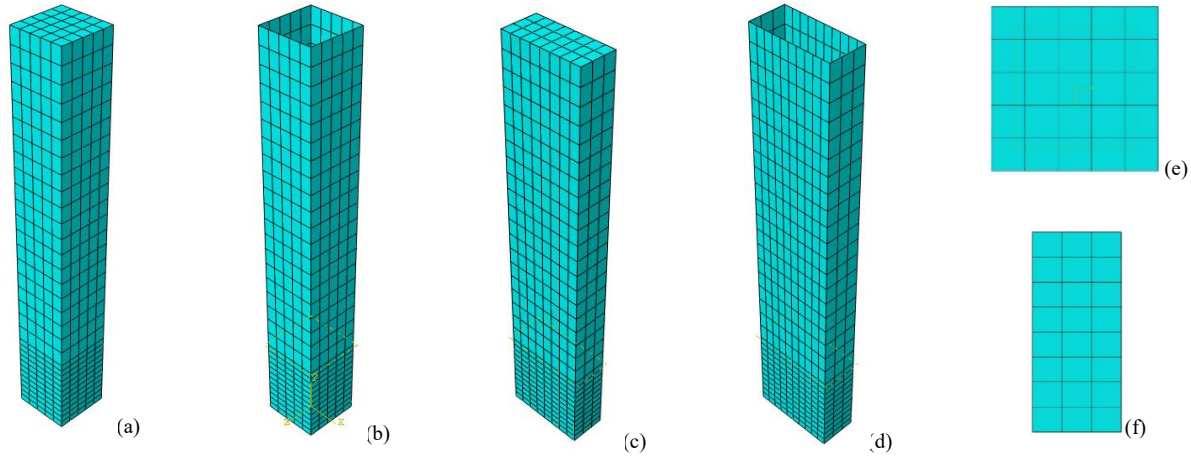

Fig 2. Mesh patterns of short columns a,c) concrete core b,d) steel tube e,f) cross-section

3. Model verification

In order to ensure the implementation of the model's parameters, the numerical results have been compared with the experimental result for the study that was conducted by Silva, Jiang [34]. As could be seen from Fig. , all the numerical results give a good agreement with experimental results. However, specimens b in Fig. presented a higher disparity between numerical and experimental results. This occurred since the experimental result of this specimen, Ru5%, showd a higher stress than Ru0%, which has no apparent reason, as Silva, Jiang [34] mentioned. Despite this specimen, the difference for columns without axial loading was 7%, while the average of columns with axial loading was 4%. Moreover, the failure mode of all specimens was at the compression side of the column due to the local buckling of the steel tube, as could be seen in Fig. 3, which showed an exact match with the experimental findings [34].

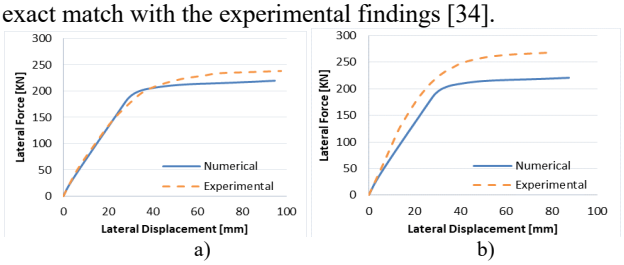

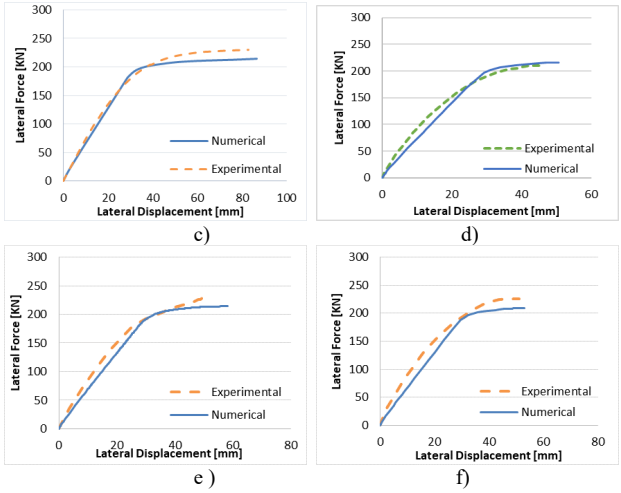

Fig. 3. Numerical vs. experimental results for 200x200x10mm CFST square columns a) M0-Ru0% b) M0-Ru5% c) M0-Ru5% d) M10-Ru0% e) M10-Ru5%CFST f) M10-Ru5%

4. Results and Discussion

4.1 Influence of rubber content

In general, the increasing of rubber replacement ratio has a marginal influence on the lateral capacity of columns as shown in Table 3 and Fig. 5, which are presented the P-u curves for square and rectangular RuCFST respectively. As could be seen there, the reduction in square columns was higher than rectangular columns. The average reduction for the square cross-section was 6% and 10% compared with 4% and 6% in rectangular cross-section for rubber content of Ru5% and Ru15% respectively. By increasing the rubber content to 5% and 15%, the reduction was 6% and 11% for slender cross-section while it was 4% and 6.5% for compacted cross-section. Eventually, the rubber replacement percentage has no significant effect on the lateral drift. These results are so far compatible with the previous findings [34, 41] in term of the strength and the lateral displacement.

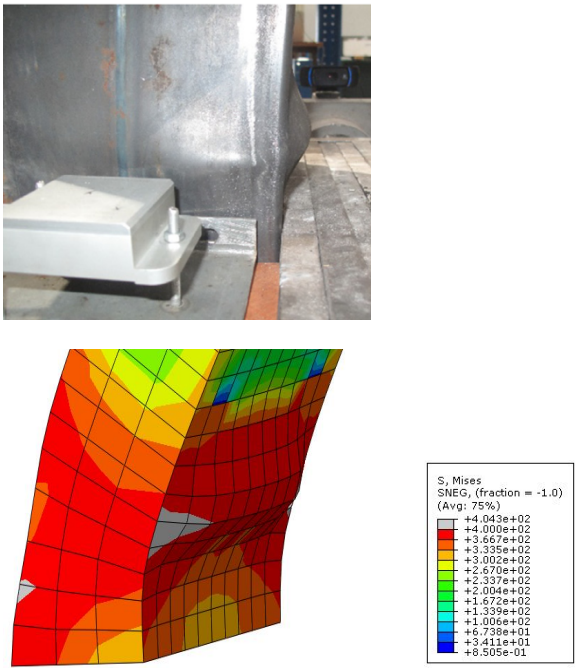

Fig. 3. Typical failure mode for column

4.2 Influence of columns' length

The increase of columns slenderness has a reverse impact on the lateral capacity of the columns. As could be seen from **Fig.** and **Fig.** , increasing the length of the column from 1500mm to 3000mm lead to decrease the columns lateral strength about 56% and 58% for square and rectangular columns respectively. These values were approximately constant at all specimens with a deviation equal to ±3.0%. Moreover, the column length lead to a significant increase on the displacement ductility. The average of this increasing for square columns were 14%, 67%, and 114%, although the average increasing for rectangular columns were 8%, 42%, and 58% for M0, M20, and M50 respectively as shown in **Fig. 4** and **Fig. 5**. A similar observations was found on literature for both deformation and capacity [42, 43].

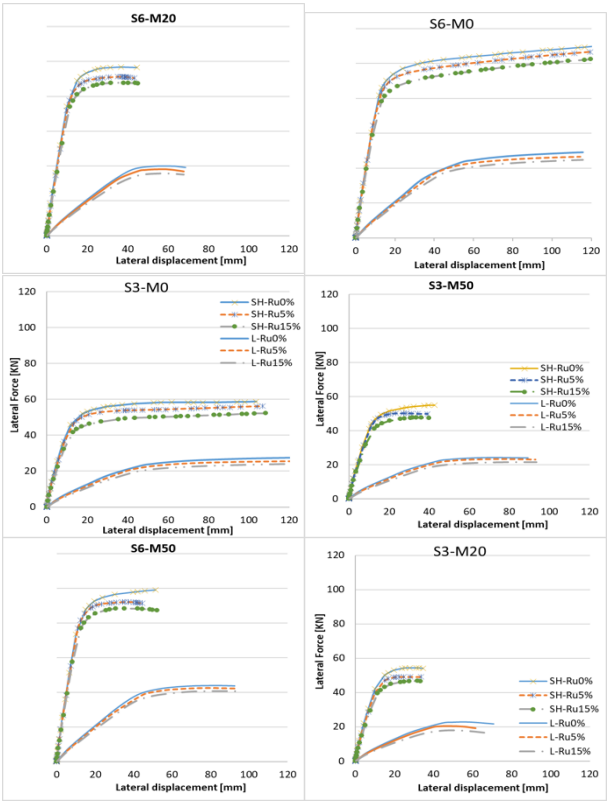

Fig. 4. P-u diagrams of square columns

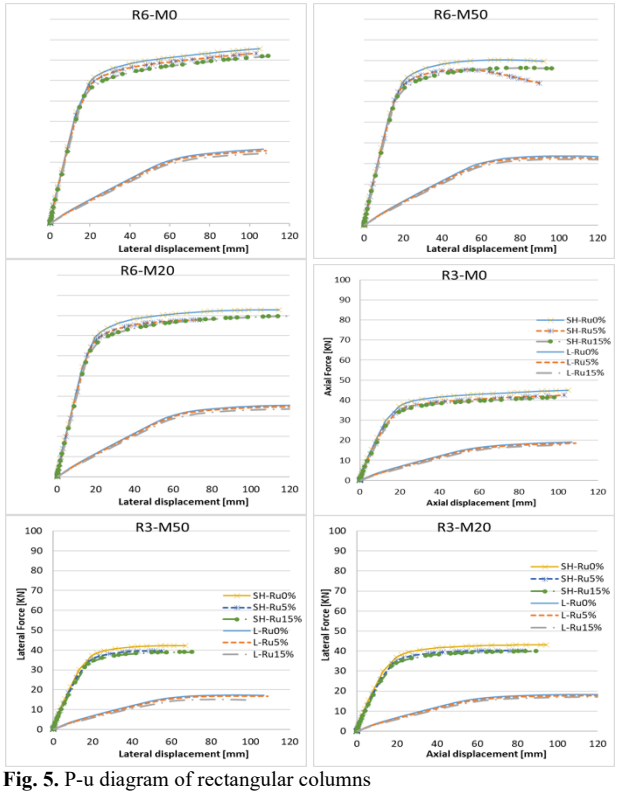

Fig. 5. P-u diagram of rectangular columns

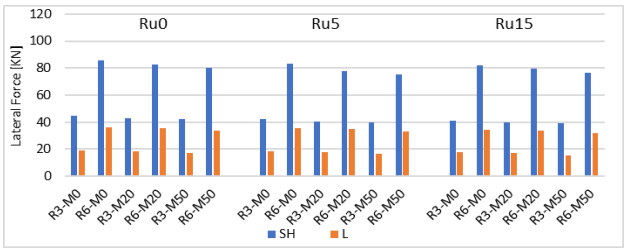

Fig. 7. influence of column length for square cross-section

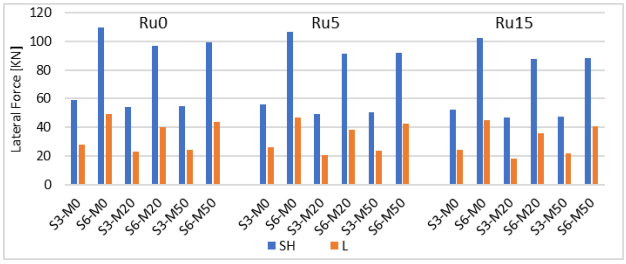

Fig. 8. influence of column length for rectangular cross-section

4.3 Influence of axial loading percentage

The results showed that axial loading level influence the columns lateral capacity. A presented in the Fig. and Fig. , the column that subjected to pure lateral force show a higher capacity than column subjected to combination loading. Additionally, increasing the axial loading leads to a decrease in the lateral drift of columns. Both reductions, in capacity and drift, occurred since in the earlier stage, when the columns start to incline, the axial loading increases the moment which accelerates the column failure. These results confirm the findings of previous studies. For instant, Chou and Wu [44] reported a reduction on lateral displacement ductility with increasing the axial load for CFST columns subjected to lateral cyclic loading. As well, Han, Wang [45] stated that ductility coefficient and energy dissipation of composite frame reduced with increase the axial load.

On the other hand, the average reduction in the square column capacity with slender cross-section was 17% and 11%, while it was 18% and 13% for compacted square columns for M20% and M50% respectively. Regarding the slender rectangular columns, the average of the reduction was 23% and 27%, although the reduction was 24% and 28% in compacted rectangular columns for M20% and M50% respectively.

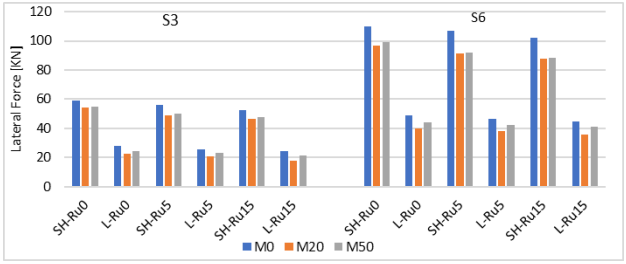

Fig. 9. Influence of axial loading percentages for square column

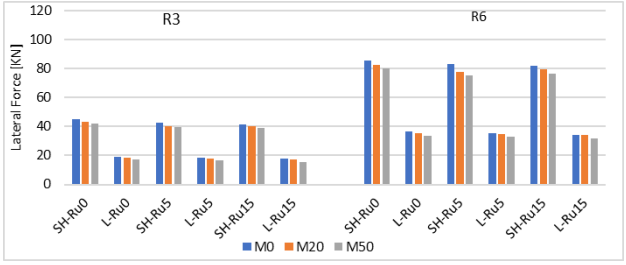

Fig. 10. Effect of axial loading percentages for rectangular column

4.4 of tube thickness

Increasing the tube thickness from 3mm to 6mm, slender and compacted cross-section respectively, caused an obvious increase in the columns' strength. The average of this increase was 46% for square and 49% for rectangular columns. Moreover, the lateral displacement was found smaller at the columns with a slender cross-section in comparison with the compacted cross-section. This occurred due to the increasing of tube thickness, which increases the steel confinement ability. That, in turn, leads to enhance the concrete performance and strengthen the column. Fig. and Fig compare the lateral capacity of compacted cross-section and slender cross-section for square and rectangular respectively. These findings are confirming the earlier results reported by Jiang, Silva [46] who reported a remarkable increasing in lateral resistance by decreasing the columns' slenderness.

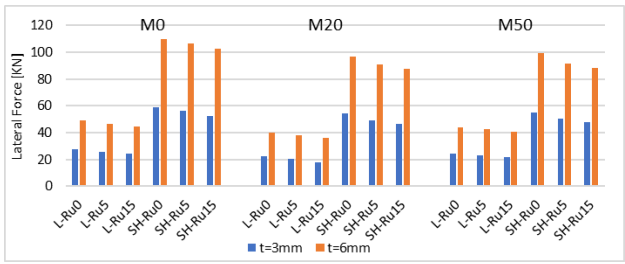

Fig. 11. The influence of the tube thickness for square columns

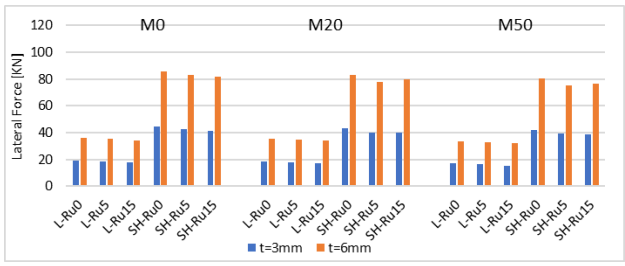

Fig 12. The influence of the tube thickness for rectangular columns

5. Conclusions

In this study, RuCFST columns modelled under several lateral monotonic loading patterns. Several parameters had been adopted including rubber content, cross-section shape and slenderness, and columns length. From the analytical investigation, the following conclusions could be drawn:

- The adopted model of columns subjected to axial force and lateral monotonic force, with and with-out constant axial force, in elastic and plastic phases, gives a good agreement between numerical and experimental results.
- Using RuCFST will expand the field of using waste tyres which will lead to reduces environmental pollution.
- Using rubber content up to 15% as a replacement of natural aggregate is recommended for both short and long CFST columns; since the increasing of rubber content has no significant effect in columns that subjected to lateral force.
- The columns length play an important role in the CFST columns behavior. Increasing the columns' length from 1500mm to 3000mm leads to decrease the column capacity under lateral loading approximately about 56% for square columns and 58% for rectangular columns. Moreover, the lateral displacement increased significantly by increasing the columns' length.
- Column's lateral capacity increase with the increasing the tube thickness, regarding the increasing of the confinement ability.
- Square columns showed higher resistance for the lateral loads than rectangular columns due to the small width of the rectangular column.

References

1. Shetty, M., *Concrete technology.* S. chand & company LTD, 2005: p. 420-453.
2. Almeshal, I., et al., *Use of recycled plastic as fine aggregate in cementitious composites: A review.* Construction and Building Materials, 2020. **253**: p. 119146.
3. Vishwakarma, V. and D. Ramachandran, *Green Concrete mix using solid waste and nanoparticles as alternatives–A review.* Construction and Building Materials, 2018. **162**: p. 96-103.
4. Silvestravičiūtė, I. and L. Šleinotaitė-Budrienė, *Possibility to use scrap tyres as an alternative fuel in cement industry.* Environmental research, engineering and management, 2002. **3**(21).
5. Taverne, J.-P., *End of life tyres-A valuable resource with growing potential.* ETRma End-of-life Tyres Management Report of, 2011.
6. Humphrey, D.H., *Civil engineering applications of chipped tires*. 1996: Manitoba Tire Stewardship Board.
7. Topcu, I.B., *The properties of rubberized concretes.* Cement and concrete research, 1995. **25**(2): p. 304-310.
8. Sgobba, S., et al. *Use of rubber particles from recycled tires as concrete aggregate for engineering applications*. in *2nd International conference on sustainable construction materials and technologies*. 2010.
9. Batayneh, M., I. Marie, and I. Asi, *Use of selected waste materials in concrete mixes.* Waste management, 2007. **27**(12): p. 1870-1876.
10. Al Rawahi, Z. and M.B. Waris. *Use of recycled tires in non-structural concrete*. in *MATEC Web of Conferences*. 2017. EDP Sciences.
11. Lv, J., et al., *Effects of rubber particles on mechanical properties of lightweight aggregate concrete.* Construction and Building Materials, 2015. **91**: p. 145-149.
12. Hajjar, J.F., *Composite steel and concrete structural systems for seismic engineering.* Journal of Constructional Steel Research, 2001.
13. Atahan, A.O. and A.Ö. Yücel, *Crumb rubber in concrete: static and dynamic evaluation.* Construction and building materials, 2012. **36**: p. 617-622.
14. Khaloo, A.R., M. Dehestani, and P. Rahmatabadi, *Mechanical properties of concrete containing a high volume of tire–rubber particles.* Waste Management, 2008. **28**(12): p. 2472-2482.
15. Khatib, Z.K. and F.M. Bayomy, *Rubberized Portland cement concrete.* Journal of materials in civil engineering, 1999. **11**(3): p. 206-213.
16. Ganjian, E., M. Khorami, and A.A. Maghsoudi, *Scrap-tyre-rubber replacement for aggregate and filler in concrete.* Construction and building materials, 2009. **23**(5): p. 1828-1836.
17. Jalal, M., N. Nassir, and H. Jalal, *Waste tire rubber and pozzolans in concrete: A trade-off between cleaner production and mechanical properties in a greener concrete.* Journal of Cleaner Production, 2019. **238**: p. 117882.
18. Issa, C.A. and G. Salem, *Utilization of recycled crumb rubber as fine aggregates in concrete mix design.* Construction and Building Materials, 2013. **42**: p. 48-52.
19. Xue, J. and M. Shinozuka, *Rubberized concrete: A green structural material with enhanced energy-dissipation capability.* Construction and Building Materials, 2013. **42**: p. 196-204.
20. Zheng, L., X.S. Huo, and Y. Yuan, *Experimental investigation on dynamic properties of rubberized concrete.* Construction and building materials, 2008. **22**(5): p. 939-947.
21. Vadivel, T.S., R. Thenmozhi, and M. Doddurani, *Experimental behaviour of waste tyre rubber aggregate concrete under impact loading.* Iranian Journal of Science and Technology. Transactions of Civil Engineering, 2014. **38**(C1+): p. 251.
22. Alshaikh, I.M., et al., *Progressive collapse of reinforced rubberised concrete: Experimental study.* Construction and Building Materials, 2019. **226**: p. 307-316.
23. Al-Tayeb, M.M., et al., *Effect of Partial Replacements of Coarse Aggregate by Polycarbonate Plastic Waste on the First Crack Impact Resistance of Concrete Beam.* 2020.
24. Pham, T.M., et al., *Dynamic compressive properties of lightweight rubberized concrete.* Construction and Building Materials, 2020. **238**: p. 117705.
25. Al-Tayeb, M.M., et al., *Effect of partial replacement of sand by recycled fine crumb rubber on the performance of hybrid rubberized-normal concrete under impact load: experiment and simulation.* Journal of cleaner production, 2013. **59**: p. 284-289.
26. M. Al-Tayeb, M., et al., *Experimental and numerical investigations of the influence of partial replacement of coarse aggregates by plastic waste on the impact load.* International Journal of Sustainable Engineering, 2020: p. 1-8.
27. Pham, T.M., et al., *Dynamic response of rubberized concrete columns with and without FRP confinement subjected to lateral impact.* Construction and Building Materials, 2018. **186**: p. 207-218.
28. Gholampour, A., et al., *Behavior of Actively Confined Rubberized Concrete under Cyclic Axial Compression.* Journal of Structural Engineering, 2019. **145**(11): p. 04019131.
29. Son, K.S., I. Hajirasouliha, and K. Pilakoutas, *Strength and deformability of waste tyre rubber-filled reinforced concrete columns.* Construction and building materials, 2011. **25**(1): p. 218-226.
30. Youssf, O., M.A. ElGawady, and J.E. Mills. *Experimental investigation of crumb rubber concrete columns under seismic loading*. in *Structures*. 2015. Elsevier.
31. Moustafa, A., A. Gheni, and M.A. ElGawady, *Shaking-table testing of high energy–dissipating rubberized concrete columns.* Journal of Bridge Engineering, 2017. **22**(8): p. 04017042.
32. Abendeh, R., H.S. Ahmad, and Y.M. Hunaiti, *Experimental studies on the behavior of concrete-filled steel tubes incorporating crumb rubber.* Journal of Constructional Steel Research, 2016. **122**: p. 251-260.
33. Duarte, A., et al., *Tests and design of short steel tubes filled with rubberised concrete.* Engineering Structures, 2016. **112**: p. 274-286.
34. Silva, A., et al., *Monotonic and cyclic flexural behaviour of square/rectangular rubberized concrete-filled steel tubes.* Journal of Constructional Steel Research, 2017. **139**: p. 385-396.
35. Silva, A., et al., *Experimental characterisation of the flexural behaviour of rubberized concrete-filled steel tubular members.* ce/papers, 2017. **1**(2-3): p. 2147-2156.
36. Nematzadeh, M., A. Karimi, and S. Fallah-Valukolaee, *Compressive performance of steel fiber-reinforced rubberized concrete core detached from heated CFST.* Construction and Building Materials, 2020. **239**: p. 117832.
37. AISC, *360-10,"Specification for Structural Steel". Chicago (IL).* 2010.
38. Simulia, *ABAQUS Standard, User's Manual, Version 6.12-1, Rhode Island, USA.* 2012.
39. Silvestre N, F.B., Lopes JNC *Compressive behavior of CNT-reinforced aluminum composites using molecular dynamics.* Composites Science and Technology 2014. **90, 16-24.**
40. Johnson, R.P. and D. Anderson, *Designers' Guide to EN 1994-1-1: Eurocode 4: Design of Composite Steel and Concrete Structures. General Rules and Rules for Buildings*. 2004: Thomas Telford.
41. Silva, A., et al., *Experimental assessment of the flexural behaviour of circular rubberized concrete-filled steel tubes.* Journal of Constructional Steel Research, 2016. **122**: p. 557-570.
42. Li, W. and L.-H. Han, *Seismic performance of CFST column to steel beam joints with RC slab: analysis.* Journal of Constructional Steel Research, 2011. **67**(1): p. 127-139.
43. Ding, F.-x., et al., *Composite frame of circular CFST column to steel-concrete composite beam under lateral cyclic loading.* Thin-Walled Structures, 2018. **122**: p. 137-146.
44. Chou, C.-C. and S.-C. Wu, *Cyclic lateral load test and finite element analysis of high-strength concrete-filled steel box columns under high axial compression.* Engineering Structures, 2019. **189**: p. 89-99.
45. Han, L.-H., W.-D. Wang, and Z. Tao, *Performance of circular CFST column to steel beam frames under lateral cyclic loading.* Journal of Constructional Steel Research, 2011. **67**(5): p. 876-890.
46. Jiang, Y., et al. *Experimental and Numerical Assessment of the Behaviour of RuCFST Members under Monotonic and Cyclic Bending*. in *Proceedings of the 16th World Conference on Earthquake Engineering, The International Association for Earthquake Engineering, 16WCEE*. 2017.